The Role of Electron-Phonon Coupling in Spin Transport through FM-QD Molecular-FM in the Presence of Spin Accumulation in the Leads

Nada K. Khassaf[1*], J.M. AL-Mukh[2]

Abstract

The spin transport process through quantum dot molecular, embedded between two ferromagnetic leads in parallel configuration with the presence of spin accumulation, is studied by getting use of the non-equilibrium Keldysh – Green's function technique. The electron-phonon coupling can be implicitly considered in the model, using the canonical transformation where a single phonon mode is considered in the strong electron – phonon coupling regime. Since the heat may interchange between the quantum dot molecular and the phonon bath coupled to it. And as the principle aim of our study is to determine the parameters that afford high spin (charge) heat generation, that must be avoid in the experimental applications, all the spin transport properties are investigated throughout the calculation of the spin and charge accumulation on the quantum dot molecular, the spin polarized currents, the spin and charge currents, the spin polarized heat generations, the spin heat generation and the charge heat generation. The calculations are accomplished as a function of the model calculation parameters that can be tuned experimentally. The spin blockade and the negative differential phenomena are investigated since the spin transport properties are studied extendedly in the case of a parallel configuration in the leads. It is concluded that the operative and functional values of the bias voltage can be determined by single phonon energy and the electron-phonon coupling values. Since all our calculations are accomplished for electron-phonon coupling equals 0.05eV.

Finally, we must report the following: in the case of parallel configuration with high spin polarization, the spin heat generation equals the charge heat generation and both are relatively high where the intradot interaction has no role. While, as the spin polarization is lowered then the charge heat generation be greater than the spin heat generation when the correlation energy is relatively low.

Key Words: Quantum Dot Molecular, Spin Accumulation in the Ferromagnetic Leads, Electron- phonon Coupling.

DOI Number: 10.14704/nq.2022.20.5.NQ22144 **NeuroQuantology 2022; 20(5):16-24**

Introduction

Mesoscopic physics can be defined as the study of quantum electronic phenomena, in the atomic domain, that are realized low dimensional nanostructures ranging from tens of nanometers up to micrometers. The heat flow in these structures had become a very interesting research topic for attractive and viable reasons [1,2]. The heat produced in such dimensions may be broken down the structures' stability. This problem leads many researchers to investigate and understand the heat generation and heat transport in nanodevices coupled to phonon bath [3]. The heat is exchanged with the environment through contact electron reservoirs and phonon bath [4].

Corresponding author: Nada K. Khassaf
Address: [1*,2]Department of Physics, College of Education for Pure Sciences, University of Basrah, Basrah, Iraq.
Relevant conflicts of interest/financial disclosures: The authors declare that the research was conducted in the absence of any commercial or financial relationships that could be construed as a potential conflict of interest.
Received: 03 March 2022 **Accepted:** 08 April 2022

The electrons or phonons in such devices are at most driven by electric bias voltage or thermal bias as well as spin bias in recent spintronic applications. So, the motion of electrons and phonons are not isolated, their interaction must be taken into consideration in studying the electron and phonon transport [5].

In 'heat' engineering applications, as the size of the electronic devices decreases to the nanoscale, the heat dissipation and conduction in these devices become pivotal issues which dramatically change the electronic properties. Many general models are needed for the role of the electron – phonon mutual interaction [6].

In our study, the nonequilibrium Green's function method is based to study and analyze the heat generation in current flow through quantum dot molecular embedded between two ferromagnetic leads, this describes the electron subsystem [7]. While the phonon subsystem is described by the phonon bath. Since it is assumed that the electron-phonon coupling is stronger than the electronic one. The heat generation, from both the electron and the phonon points of view, is studied by introducing a self-consistent solution. When the electron-phonon interaction is strong, a canonical transformation can be used to study toy models system. Therefore, the device temperature might become very high due to heat accumulation to point that the devices will not have proper function. In general, two theoretical models are considered to treat the above-mentioned system. The first treatment is accomplished by using the Density functional theoretical which models the active region and the contact regions extendedly. The second one is based on modeling takes into account all the parameters that related to the active region and leads. The theoretical treatment considered in our study is of the second type[8,9]. This treatment can investigate the extra degree of freedom such as mechanical and magnetic degree of freedom which leads to phonon and spin dynamica [10-12].

The system under consideration consists of a quantum dot molecular coupled to the left and right ferromagnetic leads (parallel configuration in the presence of spin accumulation) throughout tunnel junctions. The quantum dot molecular is also coupled to phonon bath, since the electron-phonon coupling is considered. In this study, we will determine the ascertained conditions for the operation of a quantum dot molecular with (and without) minimum heat generation.

Theoretical Description

The system under consideration is described by the following Hamiltonia [1,2]:

$$H = \sum_{k_{\alpha,\sigma}} E^{\sigma}_{k_\alpha} C^{\sigma+}_{k_\alpha} C^{\sigma}_{k_\alpha} + \sum_{\sigma}[E_d + \lambda_{ph}(C^{+}_{ph} + C_{ph})] C^{\sigma+}_{d} C^{\sigma}_{d} + U C^{\sigma+}_{d} C^{\sigma}_{d} C^{-\sigma+}_{d} C^{-\sigma}_{d} + \hbar\omega_{ph} C^{+}_{ph} C_{ph} + \sum_{k_{\alpha,\sigma}} \left(V^{\sigma}_{k_\alpha d} C^{\sigma+}_{k_\alpha} C^{\sigma}_{d} + V^{\sigma}_{dk_\alpha} C^{\sigma+}_{d} C^{\sigma}_{k_\alpha}\right) \quad (1)$$

The first term describes the left (α=L) and right (α=R) leads with $C^{\sigma+}_{k_\alpha}(C^{\sigma}_{k_\alpha})$ is the creation (annihilation) operator of an electron with momentum k, energy $E^{\sigma}_{k_\alpha}$ and spin σ.The second and third terms are related to quantum dot $C^{\sigma+}_{d}(C^{\sigma}_{d})$ creates (annihilates) an electron with energy E_d and inteadot coulomb interaction U. $C^{+}_{ph}(C_{ph})$ is the creation (annihilation) operator of a phonon having energy $\hbar\omega_{ph}$ and the quantity λ_{ph}represents electron – phonon coupling strength. The fourth term regards the single phonon mode and the last term describes the coupling interaction between the quantum dot and the leads where $V^{\sigma}_{k_\alpha d}$ represents the spin – dependent tunneling matrix element. In this treatment a canonical transformation was used to element the electron – phonon coupling terms; $\tilde{H}=\hat{X}H\hat{X}^{+}$ and the operator

$\hat{X} = \exp\left[\frac{\lambda_{ph}}{\hbar\omega_{ph}}\sum_{\sigma}\left(C^{+}_{ph} - C_{ph}\right) C^{+\sigma}_{d} C^{\sigma}_{d}\right]$ [13]. By transformation, the Hamiltonian reads:

$$\tilde{H} = \sum_{k_\alpha\sigma} E^{\sigma}_{k_\alpha} C^{\sigma+}_{k_\alpha} C_{k_\alpha} + \sum_{\sigma} \tilde{E}_d C^{\sigma+}_{d} C^{\sigma}_{d} + \tilde{U} C^{\sigma+}_{d} C^{\sigma}_{d} C^{-\sigma+}_{d} C^{-\sigma}_{d} + \sum_{k_\alpha\sigma}\left(\tilde{V}^{\sigma}_{k_\alpha d} C^{\sigma+}_{k_\alpha} C^{\sigma}_{d} + \tilde{V}^{\sigma}_{dk_\alpha} C^{\sigma+}_{d} C^{\sigma}_{k_\alpha}\right) \quad (2)$$

The quantum dot effective energy level E_d is renormalized to $\tilde{E}_d$=E_d-g $\hbar\omega_{ph}$ and the intradot correlation energy to $\tilde{U}$= U – 2g$\hbar\omega_{ph}$, with g=$(\lambda_{ph}/\hbar\omega_{ph})^2$, λ_{ph} represents the electron-phonon coupling interaction. The coupling interaction matrix element is also renormalized to $\tilde{V}^{\sigma}_{k_\alpha d} = V^{\sigma}_{k_\alpha d}$ X, with X= exp[-g(C^{+}_{ph}- C_{ph})] represents the phonon operator. And as $\lambda_{ph} > V^{\sigma}_{k_\alpha d}$, then the phonon operator can be replaced by the expectation value of X, <X>= exp[-g(N_{ph}+1/2)], where $N_{ph}(= 1/\left[exp\left(\hbar\omega_{ph}/k_B T_{ph}\right) - 1\right])$ represents the phonon distribution function. T_{ph} and k_B are the phonon bath temperature and Boltzman constant, respectively. By using Keldysh nonequilibrium technique [14-16], the transmition coefficient reads $\mathcal{T}^{\sigma}(E) = -\frac{\tilde{\Gamma}^{\sigma}_{L}\tilde{\Gamma}^{\sigma}_{R}}{\tilde{\Gamma}^{\sigma}}$ Im $\tilde{G}^{r\sigma}(E)$ and $\tilde{G}^{r\sigma}(E)$ represents the retarded green's function:

$$\tilde{G}^{r\sigma}(E) = \left\{\left[\frac{E-\tilde{E}_d-\tilde{U}((1-n_d^{\sigma})}{(E-\tilde{E}_d)(E-\tilde{E}_d-\tilde{U})}\right]^{-1} + i\frac{\tilde{\Gamma}^{\sigma}}{2}\right\}^{-1} \quad (3)$$

By calculating $\tilde{G}^{r\sigma}(E)$, the other Green's functions can be found, the advanced Green's function read as $\tilde{G}^{a\sigma}(E) = [\tilde{G}^{r\sigma}(E)]^{\star}$, the lesser Green's function $\tilde{G}^{<\sigma}(E) = \tilde{G}^{r\sigma}(E)\,\tilde{\sum}^{<\sigma}(E)\tilde{G}^{a\sigma}(E)$ and the greater Green's function $\tilde{G}^{>\sigma}(E) = \tilde{G}^{r\sigma}(E)\,\tilde{\sum}^{>\sigma}(E)\tilde{G}^{a\sigma}(E)$. Accordingly the lesser (greater) self-energy will be $\tilde{\sum}^{<\sigma}(E) = i\,[\,\tilde{\Gamma}_L^{\sigma} f_L{}^{\sigma}(E) + \tilde{\Gamma}_R^{\sigma} f_R{}^{\sigma}(E)]$ $(\tilde{\sum}^{>\sigma}(E) = -i\,[\,\tilde{\Gamma}_L^{\sigma}(1-f_L{}^{\sigma}(E)) + \tilde{\Gamma}_R^{\sigma}(1-f_R{}^{\sigma}(E))])$, where $f_{\alpha}{}^{\sigma}(E)$ is the spin dependent Fermi distribution function; $f_{\alpha}{}^{\sigma}(E) = 1/\{exp\,[E-\mu_{\alpha}^{\sigma}]/k_BT_{\alpha}+1\}$. μ_{α}^{σ} and $T_{\alpha}$are the spin dependent chemical potentials and the lead temperature, respectively. The line-width function Γ_L^{σ} means the broadening in the effective energy level of the quantum dot molecular due to coupling with the energy levels of the left and right leads; since $\Gamma_{\alpha}^{\sigma} = 2\pi\ |V_{k_{\alpha}d}^{\sigma}|^2\,\rho_{\alpha}^{\sigma}$ and the transport line width function reads $\tilde{\Gamma}_{\alpha}^{\sigma} = 2\pi\,|\tilde{V}_{k_{\alpha}d}^{\sigma}|^2\,\rho_{\alpha}^{\sigma}$ [1]. Where ρ_{α}^{σ} represents the spin dependent density of states of the ferromagnetic leads α. Accordingly, the transpose line width function reads $\tilde{\Gamma}_{\alpha}^{\sigma} = \Gamma_{\alpha}^{\sigma} < X >^2$ and the total line width function equals to $\tilde{\Gamma}^{\sigma} = \tilde{\Gamma}_L^{\sigma} + \tilde{\Gamma}_R^{\sigma}$. To calculate the hybridization function, we use the band approximation. To calculate the spin dependent electric current flows through the quantum dot, the following relation can be used [17-18].

$$I^{\sigma} = \frac{-e}{h}\int dE\,[f_L{}^{\sigma}(E) - f_R{}^{\sigma}(E)\,]\mathcal{T}^{\sigma}(E) \quad (4)$$

In order to calculate $\mathcal{T}^{\sigma}(E)$, one must firstly calculation $\tilde{G}^{r\sigma}(E)$. Accordingly, the charge current I_{ch} $(=\sum_{\sigma} I^{\sigma})$ and the spin current $I_{sp}(=\sum_{\sigma}\sigma I^{\sigma})$ can be calculated. The occupation number must be solved self consistently by using the following relation:

$$n_d^{\sigma} = -\int \frac{dE}{\pi}\left\{\frac{\Gamma_L^{\sigma} f_L{}^{\sigma}(E) - \Gamma_R^{\sigma} f_R{}^{\sigma}(E)}{\Gamma_L^{\sigma}+\Gamma_R^{\sigma}}\right\} ImG^{r\sigma}(E) \quad (5)$$

The retarded Green's function for spin σ is given by [19]:

$$G^{r\alpha}(E) = \sum_{n=-\infty}^{\infty} L_n\,\{\tilde{G}^{r\sigma}(E - n\hbar\omega_{ph}) + \frac{1}{2}\,[\tilde{G}^{<\sigma}(E - n\hbar\omega_{ph}) - \tilde{G}^{<\sigma}(E + n\hbar\omega_{ph})]\} \quad (6)$$

With,

$L_n = e^{-g(2N_{ph}+1)}\exp(n\hbar\omega_{ph}/2k_BT_{ph})J_n[(2g\sqrt{2N_{ph}(N_{ph}+1)}]$,

and $J_n(x)$ represents the modified n-th Bessel function; $J_n(x) = \sum_{m=0}^{\infty}\frac{(-1)^m}{m!(n+m)!}\left(\frac{x}{2}\right)^{n+2m}$. The occupation numbers $(n_d^{\pm\sigma})$ can be utilized to calculate the charge accumulation $A_{ch}(=\sum_{\sigma} n_d^{\sigma})$ and the spin accumulation $A_{sp}(=\sum_{\sigma}\sigma n_d^{\sigma})$ on the active region. When $T_{\alpha}=T_{ph}$ then $N_{ph}=N_{\alpha}$, the spin polarized heat generation is given by [13]:

$$Q^{\sigma} = \frac{\hbar\omega_{ph}\,\lambda_{ph}^2}{\tilde{\Gamma}_L^{\sigma}\,\tilde{\Gamma}_R^{\sigma}}\int\frac{dE}{2\pi}\,f_{LR}{}^{\sigma}(E) f_{LR}{}^{\sigma}(\tilde{E})\mathcal{T}^{\sigma}(E)\mathcal{T}^{\sigma}(\tilde{E}) \quad (7)$$

Where, $N_{\alpha} = \left[\exp\left(\frac{\hbar\omega_{ph}}{k_BT_{\alpha}}\right)-1\right]^{-1}$; $f_{LR}{}^{\sigma}(E) = f_L{}^{\sigma}(E) - f_R{}^{\sigma}(E)$ and $f_{LR}{}^{\sigma}(\tilde{E}) = f_L{}^{\sigma}(\tilde{E}) - f_R{}^{\sigma}(\tilde{E})$. Accordingly, the charge heat generation $Q_{ch}(=\sum_{\sigma} Q^{\sigma})$ and the spin heat generation $Q_{sp}(=\sum_{\sigma}\sigma Q^{\sigma})$ can also be calculated.

The Results

In the following, our results, related to the case of a parallel configuration in the presence of spin accumulation in the leads will be presented. Accordingly, the spin-dependent chemical potentials are assumed to be:

$\mu_L^{\sigma} = 0.04+eV_b$; $\mu_L^{-\sigma} = -0.04+eV_b$; $\mu_R^{\sigma} = 0.04-eV_b$; $\mu_R^{-\sigma} = -0.04-eV_b$; eV_b represents the bias voltage this means that there are two transport windows one for a spin up and the other for a spin down. The line-width function reads $\Gamma_{\alpha}^{\sigma} = \Gamma_{\alpha_o}\,(1+\sigma\,P_{\alpha})$, where σ =1(-1) for the spin-up (down) and $P_L=P_R=P$ and $0 \le P \le 1$. As the regime $V_{k_{\alpha}}^{\sigma} < \lambda_{ph}$ is considered, Γ_{α_o} and λ_{ph} are fixed at 0.003eV and 0.05eV, respectively. While the phonon mode energy and the quantum dot effective energy level are equal to 0.12eV and 0.01eV, respectively with correlation energy U=0.08 and 0.3eV. Our calculation are accomplished for spin polarization value $0.1 \le P \le 0.9$ at different values of $T_{\alpha} = T_{ph}$(=70,140,210,280k). As the temperatures of the electrons and the phonons are the same, there will be no heat conduction between the electron and the phonon subsystems, e.i. the heat generation is due to an electric current that flows through the quantum dot molecular. To determine the regime concerning the correlation, $\Gamma_{\alpha}^{\pm\sigma}$ is calculated and presented in Table (1). For U=0.3eV, the spin-up hybridization functions is in the weak correlation regime [20], $\frac{U}{\Gamma_{\alpha}^{\sigma}} < 1$, while the spin-down functions are in the strong one, $\frac{U}{\Gamma_{\alpha}^{-\sigma}} > 1$. But for U=0.08eV, the regime is weak for $P \le 0.7$ and strong for $P > 0.7$ when the spin is down. The transpose broadening function, which depends on the phonon bath temperature, electron-phonon coupling strength and the phonon mode energy, is also calculated and presented in

table (2). The value of $\tilde{\Gamma}_{\alpha}^{\sigma}$ ($\tilde{\Gamma}_{\alpha}^{-\sigma}$) increases (decreases) with spin polarization increasing. In general, we have $\tilde{\Gamma}_{\alpha}^{\sigma} >> \tilde{\Gamma}_{\alpha}^{-\sigma}$ with increasing the spin polarization. Approximately, the temperature has no role in determining the values of $\tilde{\Gamma}_{\alpha}^{-\sigma}$ and $\tilde{\Gamma}_{\alpha}^{\sigma}$, keeping in mind that $K_B T_{ph} > \tilde{\Gamma}_{\alpha}^{\sigma} > \tilde{\Gamma}_{\alpha}^{-\sigma}$ for all temperature values used in our calculations.

Table 1. The broadening functions $\Gamma_{\alpha}^{\pm\sigma}$ as function of spin polarization

p	Γ_L^{σ}=Γ_R^{σ} (10^{-2} eV)	$\Gamma_L^{-\sigma}$=$\Gamma_R^{-\sigma}$ (10^{-2} eV)
0.1	0.33	0.27
0.2	0.36	0.24
0.3	0.39	0.21
0.4	0.42	0.18
0.5	0.45	0.15
0.6	0.48	0.12
0.7	0.51	0.09
0.8	0.54	0.06
0.9	0.57	0.03

Table 2. The transposed broadening function $\tilde{\Gamma}_{\alpha}^{\pm\sigma}$ as a function of spin polarization and phonon bath temperature

p	$T_{ph} = T_{\alpha} = 70K$		$T_{ph} = T_{\alpha} = 140K$		$T_{ph} = T_{\alpha} = 210K$		$T_{ph} = T_{\alpha} = 28K$	
	$K_B T_{\alpha}$=0.603(10^{-2}eV)		$K_B T_{\alpha}$=1.206(10^{-2}eV)		$K_B T_{\alpha}$=1.809(10^{-2}eV)		$K_B T_{\alpha}$=2.412(10^{-2}eV)	
	$\tilde{\Gamma}_L^{\sigma} = \tilde{\Gamma}_R^{\sigma}$ (10^{-2}eV)	$\tilde{\Gamma}_L^{-\sigma} = \tilde{\Gamma}_R^{-\sigma}$ (10^{-2}eV)	$\tilde{\Gamma}_L^{\sigma} = \tilde{\Gamma}_R^{\sigma}$ (10^{-2}eV)	$\tilde{\Gamma}_L^{-\sigma} = \tilde{\Gamma}_R^{-\sigma}$ (10^{-2}eV)	$\tilde{\Gamma}_L^{\sigma} = \tilde{\Gamma}_R^{\sigma}$ (10^{-2}eV)	$\tilde{\Gamma}_L^{-\sigma} = \tilde{\Gamma}_R^{-\sigma}$ (10^{-2}eV)	$\tilde{\Gamma}_L^{\sigma} = \tilde{\Gamma}_R^{\sigma}$ (10^{-2}eV)	$\tilde{\Gamma}_L^{-\sigma} = \tilde{\Gamma}_R^{-\sigma}$ (10^{-2}eV)
0.1	0.27741	0. 22697	0. 27740	0. 07565	0. 27728	0. 22686	0. 27674	0. 22642
0.2	0.03262	0. 20175	0.30262	0.20175	0. 30249	0. 20166	0. 30189	0. 20126
0.3	0.32784	0. 17653	0.32784	0.17653	0. 32769	0. 17645	0. 32705	0. 17610
0.4	0.35306	0. 15131	0. 35306	0.15131	0. 35290	0. 15124	0. 35221	0. 15095
0.5	0.37828	0. 12609	0. 37827	0. 12609	0. 37811	0. 12604	0. 37737	0. 12579
0.6	0.40350	0. 10087	0. 40349	0. 10087	0. 40331	0. 10083	0. 40252	0. 10063
0.7	0.42872	0. 07565	0. 42871	0. 22696	0. 42852	0.075621	0. 42768	0.07547
0.8	0.45394	0. 05043	0. 45393	0.050437	0. 45373	0.05041	0. 45284	0.05031
0.9	0. 47916	0.02521	0. 47915	0.025218	0. 47894	0.02520	0. 47800	0.02515

For the importance of spin accumulation and charge accumulation in the quantum dot, especially for the role of electron-phonon coupling in quantum computing, both are presented in figures (1) and (2) a function of bias voltage for different values of U and P with $T_{\alpha} = T_{ph}$=70K. It is noticed that the values of A_{ch} and A_{sp} are equal for $-\lambda_{ph} < eV_b < \lambda_{ph}$, this means $n_d^{-\sigma} \cong 0$. In figures (1a) and (2a), two peaks appear at $eV_b = \pm\hbar\omega_{ph}$ when U equals to 0.3eV for all values of spin polarization. By reducing the charging energy to 0.08eV, the physical features will be varied but the spin accumulation values will be negative (i.e. $n_d^{-\sigma} > n_d^{\sigma}$), when P=0.1 for $eV_b > |2\hbar\omega_{ph}|$. Fig.(3) represents the spin-polarized currents I^{σ} and $I^{-\sigma}$ as a function of bias voltage when U=0.3eV. I^{σ} and $I^{-\sigma}$ show step-like behavior, but there is a reduction in the values of I^{σ} at $\hbar\omega_{ph} < eV_b < 2\hbar\omega_{ph}$. The physical features (for I^{σ} and $I^{-\sigma}$) are counteractive when the polarity of the bias voltage be negative. When U=0.08eV, one can notice different behavior. I^{σ} and $I^{-\sigma}$ show linear relation for positive value of $\frac{1}{2}\lambda_{ph} < eV_b < \lambda_{ph}$ as well as $eV_b < \lambda_{ph}$. Also, one can see $I^{\sigma} \gg I^{-\sigma}$ with increasing the spin polarization to 0.9, since the correlation energy has no role in determining the values of $I^{-\sigma}$ (see fig.(4)). Figures (5-6) determine the behavior of spin and charge current with bias voltage. For both values of U, $I_{ch} > I_{sp}$ when P=0.1. Since, the spin current (charge current) does (not) show a negative differential. With increasing the spin polarization, where as $\tilde{\Gamma}_{\alpha}^{\sigma} >> \tilde{\Gamma}_{\alpha}^{-\sigma}$, the spin current equals the charge current, this referes to $I^{-\sigma} \cong 0$. Fig. (5a) shows a negative differential in the spin current curve at $eV_b = \hbar\omega_{ph}$ and $eV_b = 2\hbar\omega_{ph}$ at relatively high correlation energy. Since the width of the negative differential increases with bias voltage. At U=0.08eV, the negative differential is at $eV_b = \lambda_{ph}$ only, with increasing the spin polarization, no negative differential can be noticed. Figures (7-8) represent the spin-polarized heat generation Q^{σ} and $Q^{-\sigma}$ as a function of bias voltage. It is found that Q^{σ} is nearly equal to $Q^{-\sigma}$ when P=0.1, but with increasing the spin polarization in the leads, we have $Q^{\sigma} \gg Q^{-\sigma}$. This can be attributed to the inequality in the tunnel coupling with the leads.

The spin up polarized heat generation also shows negative differential when U=0.3eV. One of the most important phenomena is the spin blockade in Q^{σ} and $Q^{-\sigma}$ curves at the values of the bias voltage that are lying about $eV_b = 0$. The over mentioned physical notes can be found also in figs. (9) and (10) concerning the spin heat generation and charge heat generation.

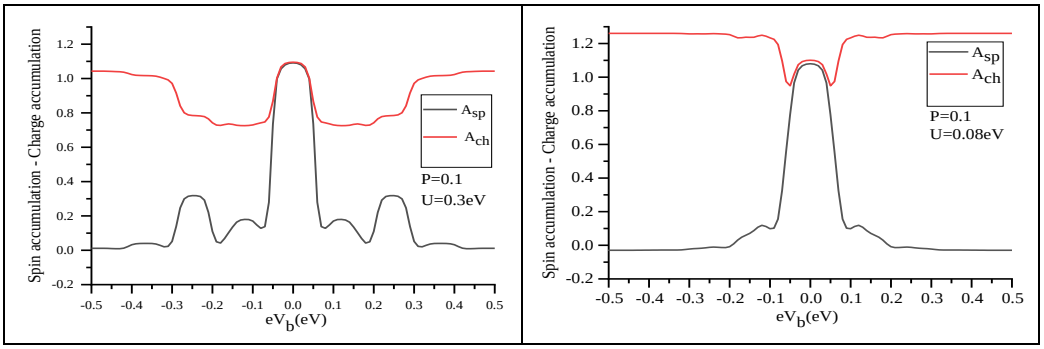

Figure 1. A_{sp} and A_{ch} as a function of eV_b when P=0.1 and U=0.3,0.08eV

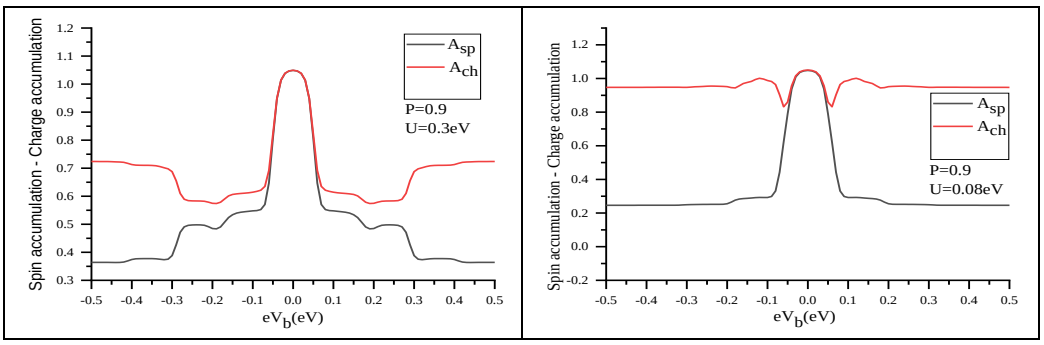

Figure 2. A_{sp} and A_{ch} as a function of eV_b when P=0.9 and U=0.3, 0.08eV

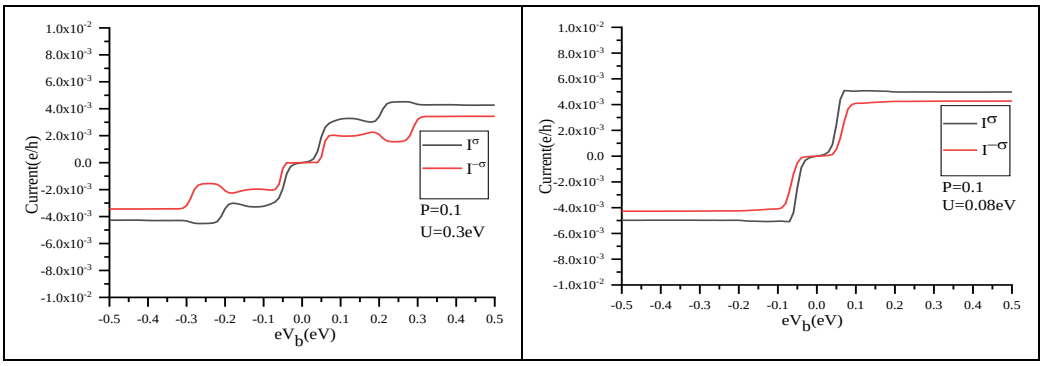

Figure 3. I^{σ} and $I^{-\sigma}$ as a function of eV_b when P=0.1 and U=0.3,0,08eV

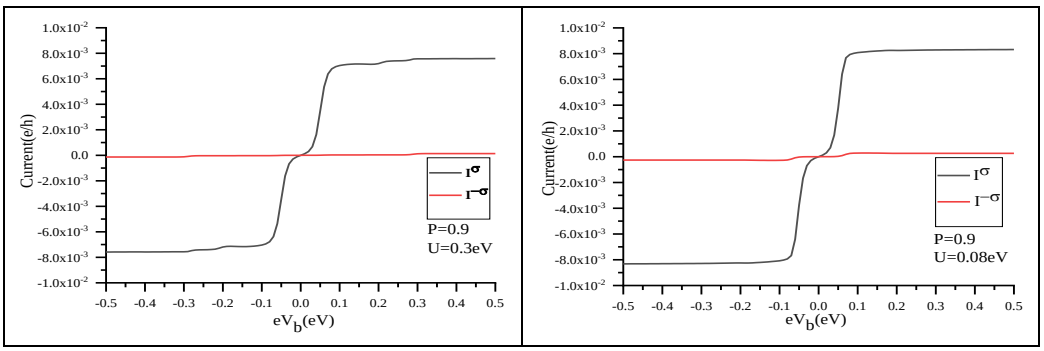

Figure 4. I^{σ} and $I^{-\sigma}$ as a function of eV_b when P=0.9 and U=0.3,0.08eV

eISSN 1303-5150

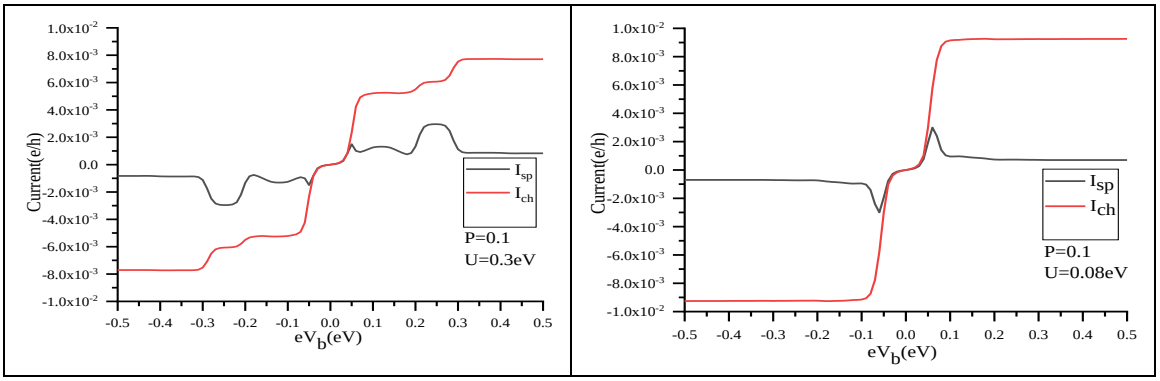

Figure 5. I_{sp} and I_{ch} as a function of eV_b when *P*=0.1 and U=0.3,0.08eV

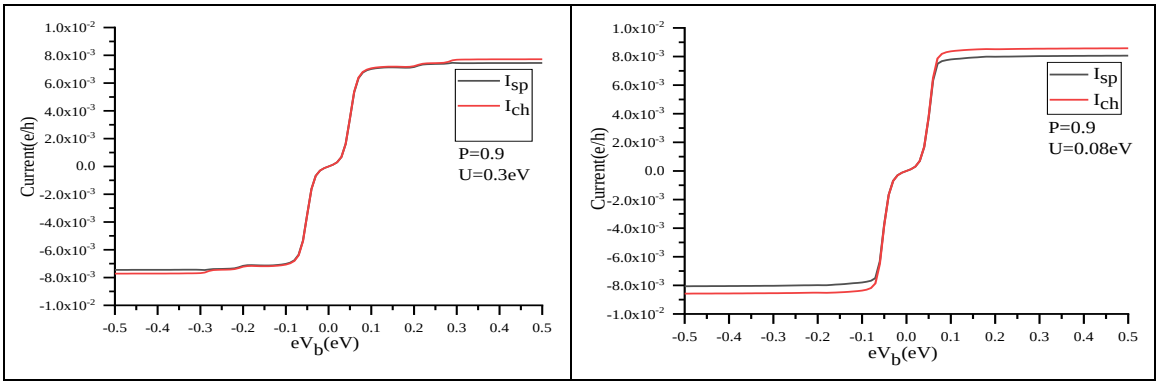

Figure 6. I_{sp} and I_{ch} as a function of eV_b when *P*=0.9 and U=0.3,0.08eV

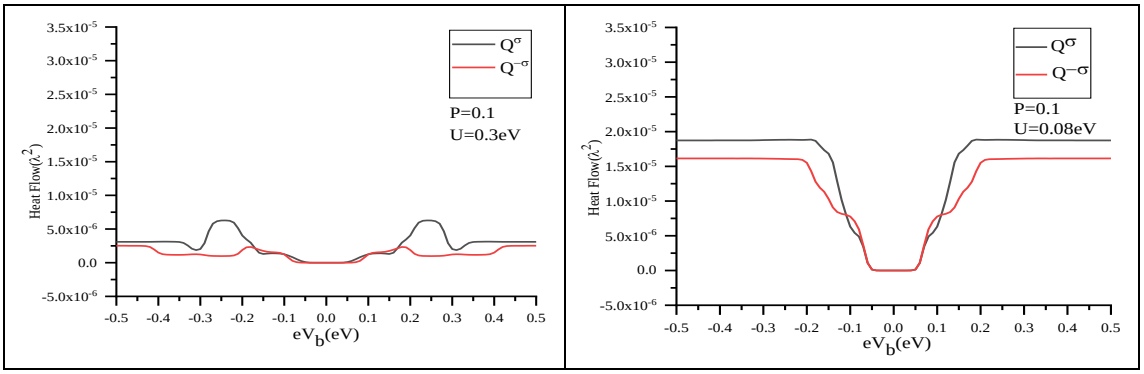

Figure 7. Q^{σ} and $Q^{-\sigma}$ as a function of eV_b when *P*=0.1 and U=0.3,0.08eV

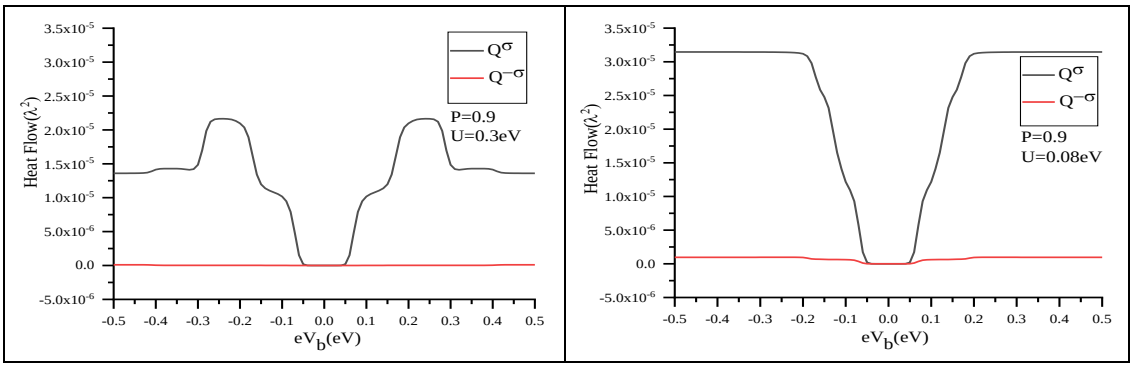

Figure 8. Q^{σ} and $Q^{-\sigma}$ as a function of eV_b when *P*=0.9 and U=0.3,0.08eV

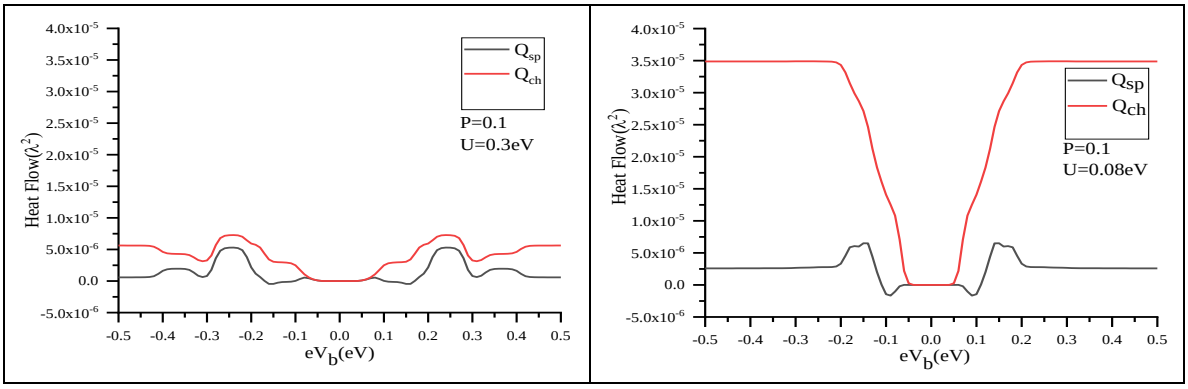

Figure 9. Q_{sp} and Q_{ch} as a function of eV_b when *P*=0.1 and U=0.3,0.08eV

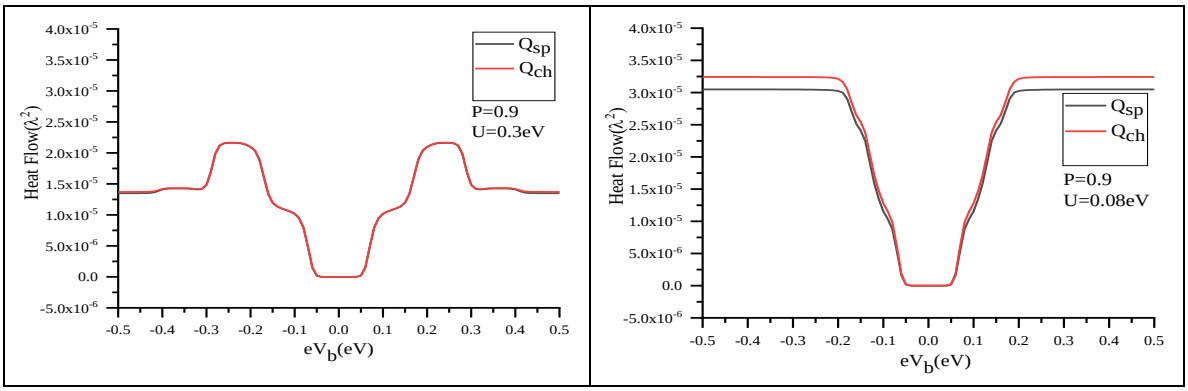

Figure 10. $Q_{sp}$and Q_{ch} as a function of $eV_b$when *P*=0.9 and U=0.3,0.08eV

There figures show a negative differential when U=0.3eV for spin and charge heat generation for both values of spin polarization. With reducing the correlation energy to 0.08eV, a negative differential emerges in spin heat generation when *P*=0.1.

To investigate the role of temperature ($T_{ph} = T_{\alpha}$) in determining the spin and charge transport properties, our calculations are accomplished for 140,210,280K and $0.1 \leq P \leq 0.9$. The physical features of our results are summarized in tables (3-6). Table (3), presents the width (i.e the values of eV_b) of spin-down blockade region for $I^{-\sigma}$ that emerges only for *P*=0.8 and 0.9 when U=0.3eV. Table (4) represents our results for Q^{σ}. For certain value of T_{α}=T_{ph}, the spin blockade width is constant for different value of spin polarization. While, for certain value of *P*, the width decreases with rising temperature. No role for the correlation energy is show in Table (4).

Table 3. The width of the spin blockade region in the spin-down polarized current as a function of spin polarization, electrodes temperature and correlation energy

P	U=0.3 eV				U=0.08 eV			
	The width of the spin blockade region(eV)				The width of the spin blockade region(eV)			
	70K	140K	210K	280K	70K	140K	210K	280K
0.1	---	---	---	---	---	---	---	---
0.2	---	---	---	---	---	---	---	---
0.3	---	---	---	---	---	---	---	---
0.4	---	---	---	---	---	---	---	---
0.5	---	---	---	---	---	---	---	---
0.6	---	---	---	---	---	---	---	---
0.7	---	---	---	---	---	---	---	---
0.8	0.02	0.04	0.02	---	---	---	---	---
0.9	0.06	0.04	0.02	---	---	---	---	---

Table 4. The width of the spin blockade region in the spin-up heat generation as a function of spin polarization, electrodes temperature and correlation energy

P	U=0.3 eV				U=0.08 eV			
	The width of the spin blockade region (eV)				The width of the spin blockade region(eV)			
	70K	140K	210K	280K	70K	140K	210K	280K
0.1	0.08	0.06	0.04	0.02	0.08	0.06	0.04	0.02
0.2	0.08	0.06	0.04	0.02	0.08	0.06	0.04	0.02
0.3	0.08	0.06	0.04	0.02	0.08	0.06	0.04	0.02
0.4	0.08	0.06	0.04	0.02	0.08	0.06	0.04	0.02
0.5	0.08	0.06	0.04	0.02	0.08	0.06	0.04	0.02
0.6	0.08	0.06	0.04	0.02	0.08	0.06	0.04	0.02
0.7	0.08	0.06	0.04	0.02	0.08	0.06	0.04	0.02
0.8	0.08	0.06	0.04	0.02	0.08	0.06	0.04	0.02
0.9	0.08	0.06	0.04	0.02	0.08	0.06	0.04	0.02

Table 5. The width of the spin blockade region in the spin down polarized heat generation as a function of spin polarization, electrodes temperature and correlation energy

P	U=0.3 eV				U=0.08 eV			
	The width of the spin blockade region(eV)				The width of the spin blockade region(eV)			
	70K	140K	210K	280K	70K	140K	210K	280K
0.1	0.14	0.12	0.12	0.12	0.08	0.06	0.04	0.02
0.2	0.14	0.12	0.12	0.12	0.08	0.06	0.04	0.04
0.3	0.14	0.14	0.14	0.14	0.08	0.06	0.04	0.04
0.4	0.14	0.14	0.14	0.14	0.08	0.06	0.04	0.04
0.5	0.16	0.14	0.14	0.16	0.10	0.06	0.04	0.04
0.6	0.16	0.16	0.16	0.18	0.10	0.06	0.06	0.04
0.7	0.18	0.18	0. 2	0.22	0.10	0.08	0.06	0.04
0.8	0.76	0.72	0.86	0.64	0.10	0.08	0.06	0.06
0.9	0.84	0.88	0.92	0.96	0.10	0.10	0.08	0.08

Table 6. The width of the negative differential region in the spin current I_{sp} as a function of spin polarization and temperature leads and correlation energy

P	U=0.3 eV				U=0.08 eV			
	The width of the negative differential region(eV)				The width of the negative differential region(eV)			
	70K	140K	210K	280K	70K	140K	210K	280K
0.1	0.25-0.31	0.25-0.33	0.25-0.41	0.25-0.42	0.06-0.09	0.06-0.25	0.06-0.24	0.07-0.26
0.2	0.26-0.31	0.25-0.33	0.25-0.41	0.25-0.41	0.06-0.09	0.06-0.28	0.07-0.29	0.07-0.28
0.3	0.26-0.31	0.25-0.33	0.25-0.39	0.25-0.41	0.06-0.09	0.07-0.28	0.07-0.28	0.07-0.26
0.4	0.26-0.31	0.25-0.32	0.25-0.39	0.25-0.41	0.06-0.09	0.07-0.21	0.07-0.22	0.08-0.23
0.5	0.26-0.31	0.25-0.32	0.25-0.41	0.25-0.41	0.06-0.09	0.07-0.2	0.08-0.21	---
0.6	0.26-0.31	0.25-0.32	0.25-0.36	0.25-0.37	0.07-0.09	0.07-0.27	---	---
0.7	0.27-0.31	0.26-0.32	0.25-0.39	0.25-0.38	0.07-0.09	---	---	---
0.8	0.27-0.31	---	0.26-0.35	---	---	---	---	---
0.9	---	---	---	---	---	---	---	---

Conclusions

Our results confirm that it is conceivable to functionalize the spin polarization and spin accumulation in the leads in the case of parallel configuration, the electron-phonon coupling, the phonon mode energy and the leads temperature as well as the intradot correlation function on the quantum dot molecular site to develop the spin engineering for the nanostructures coupled to environment. Even coherences between many levels

are realized in molecule or quantum dot molecular. Common among these systems are coherences-induced transport signatures such as negative differential and Coulomb blockade, making these systems operative for technological application in spin electronic. These results can be interpreted to determine the parameters that can be adjusted and utilized to use the device as refrigerator.

References

A.A. Aligia, D. Perez Daroca, Liliana Arrachea, and P. Roura-Bas, Heat current across a capacitively coupled double quantum dot, *Phys. Rev. B,* Vol. 101, Iss. 7 -15, (2020).

M. Pustilnik and L.I. Glazman, Kondo Effect in Real Quantum Dots, *Phys. Rev. letters,* Vol. 87, No. 21, (2001).

Maxim Dzero and Jorg Schmalian, Superconductivity in Charge Kondo Systems, *Phys. Rev. letters,* Vol. 94, Iss. 15-22, (2005).

Daniel Malz and Andreas Nunnenkamp, Current rectification in a double quantum dot through fermionic reservoir engineering, *Phys. Rev. B,* Vol. 97, 165308, (2018).

L.D. Hicks and M.S. Dresselhaus, Effect of quantum-well structures on the thermoelectric figure of merit, *Phys. Rev. B,* Vol. 47, Iss. 19-15, (1993).

Shunjiang You, Daxing Xiong, and Jiao Wang, Thermal rectification in the thermodynamic limit, *Phys. Rev. E,* Vol. 101, (2020).

Feng Chi, Lian-Liang Sun, and Yu Guo, Heat generation by electronic current in a quantum dot spin-valve, *J. of Applied Phys.,* vol. 116, No. (16), (2014).

Vinitha Balachandran,Stephen R. Clark, John Goold, and Dario Poletti, Energy Current Rectification and Mobility Edges, *Phys. Rev. letters,* Vol. 123, (2019).

T Motz, M Wiedmann, JT Stockburger and J Ankerhold, Rectification of heat currents across nonlinear quantum chains: a versatile approach beyond weak thermal contact, *New J. Phys.,* Vol. 20, (2018).

M.A. Najdi, J.M. AL-Mukh, H.A. Jassem, Model Parameterization for Coherent Manipulation in Spin Current through FM-QD1-QD2-FM, *J. Phys. Conf. Ser.,* Vol. 1818, (2021).

M.A. Najdi, J.M. AL-Mukh, H.A. Jassem, Theoretical Investigation in Coherent Manipulation throughout the Calculation of the Local Density of States in FM-DQD-FM Device, *J. Materials Science Forum,* Vol. 1039, (2021).

M.A. Najdi, J.M. AL-Mukh, H.A. Jassem, Heat current across double quantum dots in series coupled to ferromagnetic leads in antiparallel configuration within weak interdot coupling regime, *J. Comput. Electron.,* Vol. 20, (2021).

Guo Yu, Sun Lian-Liang, CHI Feng, Heat Generation by Electric Current in a Quantum Dot Molecular Coupled to Ferromagnetic Leads, Commun. *Theor. Phys.,* 62(3), (2014).

F. Chi, J. Zheng, Y.S. Liu, and Y. Guo, Refrigeration effect in a single-level quantum dot with thermal bias, *J. Appl. Phys. Lett.,* vol. 100, (2012).

David M.T. Kuo and Yia-chung Chang, Thermoelectric and thermal rectification properties of quantum dot junctions, *Phys. Rev B,* Vol. 81, (2010).

David M.T. Kuo, and Yia-chung Chang, Long-distance coherent tunneling effect on the charge and heat currents in serially coupled triple quantum dots, *Phys. Rev B,* Vol. 89, (2014).

Zuo-Zi Chen, Rong Lü, and Bang-fen Zhu, Effects of electron-phonon interaction on nonequilibrium transport through a single-molecule transistor, *Phys. Rev B,* Vol. 71, (2005).

J.S. Wang, J. Wang, and J.T. Lu, Quantum thermal transport in nanostructures, *Eur. Phys. J.* B 62, 381–404, (2008).

Feng Chi, Lian-Liang Sun, Jun Zheng Yu Guo, Heat generation by spin-polarized current in a quantum-dot spin battery, *Phys. Letters A,* Vol. 379, Issue 6, (2015).

T.A. Costi and V. Zlatic, Thermoelectric transport through strongly correlated quantum dots, *J. Phys. Rev B,* 81, No. 235127, (2010).